PROCEEDINGS B

Muscle-spring dynamics in time-limited, elastic movements

Journal:	*Proceedings B*
Manuscript ID	RSPB-2016-0393
Article Type:	Research
Date Submitted by the Author:	20-Feb-2016
Complete List of Authors:	Rosario, Michael; Duke University, Biology Sutton, Gregory; University of Cambridge, Zoology Patek, Sheila; Duke University, Biology Sawicki, Gregory; North Carolina State Universityand University of North Carolina - Chapel Hill, Joint Department of Biomedical Engineering
Subject:	Biomechanics < BIOLOGY, Computational biology < BIOLOGY, Physiology < BIOLOGY
Keywords:	muscle-spring interaction, elastic energy storage, muscle dynamics, time-limited loading, fixed-end contraction, spring stiffness
Proceedings B category:	Biomechanics

Muscle-spring dynamics in time-limited, elastic movements

M.V. Rosario[1+], G.P. Sutton[2], S.N. Patek[1], and G.S. Sawicki[3]

[1]Department of Biology, Duke University, Durham, NC, U.S.A.

[2]School of Biological Sciences, University of Bristol, Bristol, U.K.

[3]Joint Department of Biomedical Engineering, North Carolina State University and University of North Carolina at Chapel Hill, Raleigh, NC, U.S.A.

[+]Corresponding author:

M. V. Rosario

Department of Ecology and Evolutionary Biology

Brown University

Providence, RI 02912 U.S.A.

Telephone: (408) 372 – 7015

Email: michael_rosario@brown.edu

Abstract (max 200 words)

Slow muscle contractions allow muscles to produce maximal force and store the most elastic energy in series springs. However, time constraints, such as those experienced during escape and predation behaviors, may prevent animals from fully contracting their muscles during spring loading. Here we ask whether animals that have limited time for elastic energy storage operate with springs that are tuned to sub-maximal muscle contractions. To answer this question, we used a dynamic model of a muscle-spring system undergoing a fixed-end contraction, with parameters from a time-limited spring-loader (bullfrog: *Lithobates catesbeiana*) and a non time-limited spring-loader (grasshopper: *Schistocerca gregaria*). We found that when muscles have less time to contract, stored elastic energy is maximized with lower spring stiffness (quantified as spring constant). The spring stiffness measured in bullfrog tendons permitted less elastic energy storage than was predicted by a modeled, maximal muscle contraction. However, when muscle contractions were modeled using biologically-relevant loading times for bullfrog jumps (50 ms), tendon stiffness actually maximized elastic energy storage. In contrast, grasshoppers, which are not time limited, exhibited spring stiffness that maximized elastic energy storage when modeled with a maximal muscle contraction. These findings demonstrate the significance of evolutionary variation in tendon and apodeme properties to realistic jumping contexts and the importance of considering the effect of muscle dynamics and behavioral constraints when considering energy storage in muscle-spring systems.

Keywords: muscle-spring interaction, elastic energy storage, muscle dynamics, time-limited loading, fixed-end contraction, spring stiffness

Introduction

Muscle contractile force is transmitted to skeletal structures through elastic structures, inextricably coupling muscle and spring dynamics. Many animals utilize muscles to temporarily store energy in their springs, such as tendons, and the stored energy can be recovered later to help power movement. The time available for muscles to load in-series springs is important because stored elastic energy is proportional to force and muscle force declines with contraction velocity (Hill 1938). Some animals store elastic energy over long time periods prior to movement (Ritzmann 1973; Ritzmann 1974; Burrows 2007) while others use power amplification systems with time-limited storage phases (Zajac 1989; Zajac and Gordon 1989; Wilson et al. 2003).

Given that the time available for spring-loading varies across animals and movement types, the relationship between spring properties such as spring stiffness (defined as spring constant in this study) and muscle-loading dynamics may impact performance (Fig. 1). For example, animals that do not have enough time to fully load their springs before the onset of movement could maximize elastic energy storage for submaximal muscle contractions. Few studies have examined the evolutionary variation of spring properties (Patek et al. 2013; Rosario and Patek 2015), yet the diversity of elastic systems suggests a range of mechanical, functional and behavioral influences on their form and function.

Here we test whether and how springs are tuned differently to permit maximal energy storage for time-limited, sub-maximal muscle contractions versus non-time limited, maximal muscle contractions. We developed a dynamic muscle-spring simulation of a fixed end contraction (Fig. 1) and used it to compare time-limited (bullfrog: *Lithobates catesbeiana*) and non-time limited (grasshopper: *Schistocerca gregaria*) jumping systems. Both frogs and grasshoppers require elastic elements to achieve their high power jumping performance (Bennet-Clark 1975; Marsh and John-Alder 1994; Peplowski and Marsh 1997; Roberts and Marsh 2003). Bullfrogs exhibit time-limited jumps in which a fast response is necessary, whereas grasshoppers perform longer-term muscle contractions in

advance of movement and thus are less impacted by time limitations. We used existing, published data from these muscle-spring systems (Bennet-Clark 1975; Azizi and Roberts 2010; Sawicki, Sheppard, et al. 2015) to simulate spring loading over a range of allowable storage times. We addressed the following two questions: 1) How does variation in the time available for muscle contraction influence the amount of energy stored in springs with different stiffness? 2) Do the values of spring stiffness of bullfrogs and grasshoppers maximize energy storage given the distinct loading regimes of their jumping behavior?

Methods

We ran simulations of bullfrog and grasshopper muscle-spring systems with varying spring stiffness' ($k_{simulation}$) and determined which $k_{simulation}$ resulted in maximal energy storage (k_{maxE}). We chose to focus on spring stiffness because this single value determined the relationship between force and spring stretch. We omitted the duration of muscle contraction using static models and included the duration of muscle contraction using dynamic models. After all simulations were run, we compared published results of spring stiffness from bullfrog tendons ($k_{bullfrog}$) and grasshopper apodeme-cuticular springs ($k_{grasshopper}$) with the results of the simulations. Below, we outline how the simulations predicted energy storage in muscle-spring systems as a function of $k_{simulation}$.

Two factors, spring stretch (Δx_s) and spring stiffness ($k_{simulation}$), were required in order to calculate stored energy:

$$Energy = \frac{1}{2} k_{simulation} \Delta x_s^2 \quad (1)$$

Determining Δx_s was complicated by the interaction between muscle and spring. For example, an increase in $k_{simulation}$ suggested higher energy storage (Eq. *1*); but, springs with higher values of $k_{simulation}$ stretch less for a given muscle force. Consequently, it was possible to increase $k_{simulation}$ such that the resulting decrease in Δx_s reduced stored energy. Therefore, to account for the interactions between

muscle and spring, we developed the following muscle-spring model.

Muscle-spring model

We simulated dynamics within muscle-spring systems by connecting, in series, a model of a muscle to a model of a spring (Fig. 1). Specifically, we connected a Hill-type muscle to a Hookean spring (Hill 1938; Zajac 1989; Winters 1990). We kept the muscle properties stiffness across all simulations while varying the spring stiffness, $k_{simulation}$. Muscle and spring models were mathematically connected and implemented in R (version 3.2.1, Vienna, Austria). In the following sections, we will explain how different instances of the model were used to predict force and elastic energy storage over a range of contraction scenarios.

Hill-type muscle model

We used a Hill-type muscle model to predict muscle force as a function of three factors: muscle length, muscle velocity, and muscle activation (Zajac 1989). The relative contributions to muscle force by these three factors are described by Equations *2 - 4*:

$$F_{length}(\Delta x_m, L_0, a_L, b_L, s) = e^{-\left(\left|\frac{\left(\left(\frac{\Delta x_m}{L_0}\right)^{b_L}\right)-1}{s}\right|\right)^{a_L}} \quad (2)$$

$$F_{velocity}(v, a_v, b_v) = \frac{1-\frac{v}{v_{max}}}{1+\frac{v}{v_{max}/4}} \quad (3)$$

$$F_{activation}(t_{contraction}, r_{act}) = \begin{cases} k_{act} \cdot t_{contraction} : r_{act} \cdot t_{contraction} < 1 \\ 1 : r_{act} \cdot t_{contraction} \geq 1 \end{cases} \quad (4)$$

where Δx_m is the distance that the muscle contracted; L_o is the muscle rest length, a_L, b_L, and s are phenomenological parameters that were fitted to describe the shape of the muscle's length-tension curve; v is muscle shortening velocity ($\Delta x_m/\Delta t$); v_{max} is the maximum shortening velocity of muscle

contraction; $t_{contraction}$ is the time the muscle has been contracting; and r_{act} is the linear rate of muscle activation. We used each of these three functions in the Hill-type muscle model to scale maximum force production; therefore, these functions evaluated from 0 to 1 and represented the fraction of maximum force that was produced by a single component (i.e., length, velocity, or activation) independent of all others (Fig. 2).

Each of the factors impacting muscle force production were combined to estimate muscle force (F_{muscle}) by multiplying the results of Eq. ***2 - 4*** with each other and the maximum tetanic force of the muscle (F_{max}):

$$F_{muscle} = F_{max} \cdot F_{length} \cdot F_{velocity} \cdot F_{activation} \quad (5)$$

In this model, maximum tetanic force was generated when each of the constituent effects on muscle force (F_{length}, $F_{velocity}$, and $F_{activation}$) equaled 1.

Hookean spring model

We represented the series elastic component of the muscle-spring model with a linear, Hookean spring. Although biological springs are not Hookean, many springs, including those of bullfrogs and grasshoppers, approximate linear force-displacement behavior over a significant region of the curve (Hollinger 2011, Bennet-Clark 1975). For this model, spring force was determined only by the displacement through which it is stretched (Δx_s) and the spring stiffness ($k_{simulation}$):

$$F_{spring} = -k_{simulation}\Delta x_s \quad (6)$$

Static muscle-spring model

We allowed the muscle and spring models to interact by setting two groups of variables equal: F_{muscle} equaled F_{spring}, and the muscle shortening length change equaled the negative of spring stretch length change (i.e., $\Delta x_m = -\Delta x_s$; see Fig. 1 for schematic):

$$F_{max} \cdot F_{length}(\Delta x_m, L_0, a_L, b_L, s) \cdot F_{velocity}(v, v_{max}) \cdot F_{activation}(t_{contraction}, r_{act}) \quad = \quad -k_{simulation}\Delta x_s \quad (7)$$

To simplify the model, variables that described muscle properties (i.e., were only used to determine the shape of the Hill-type muscle components) were held constant for a given muscle. We further simplified Eq. *7* to represent a static, steady-state solution by setting the dynamic components ($F_{activation}$ and $F_{velocity}$) to 1:

$$F_{max} \cdot F_{length}(\Delta x, L_0, a_L, b_L, s) = -k_{simulation}\Delta x \quad (8)$$

with $\Delta x = \Delta x_m = -\Delta x_s$.

Solving for Δx in Eq. *8* resulted in the maximum internal stretch of that particular spring by its in-series muscle. This value was used to calculate maximum stored elastic energy in the static simulations, the case in which contraction time to store spring energy is not limited (see Fig. 1 for schematic).

Dynamic muscle-spring model

The dynamic muscle-spring model was identical to the static model with one exception: we did not set $F_{activation}$ and $F_{velocity}$ equal to 1 in Eq. *7*. Holding all muscle properties constant and considering velocity as Δx_m and Δt resulted in the dynamic model:

$$F_{max} \cdot F_{length}(\Delta x, L_0, a_L, b_L, s) \cdot F_{velocity}(\Delta x, \Delta t) \cdot F_{activation}(t_{contraction}, r_{act}) \quad = \quad -k_{simulation}\Delta x_s \quad (9)$$

154

155 Solving for Δx at each time step was complicated by the relationship between muscle length
156 and contraction velocity. This was because Δx_m affected muscle force in two ways. First, Δx_m affected
157 F_{length} directly; values of $\frac{\Delta x_m}{L_0}$ smaller than 1 (as a result of muscle shortening contraction) decreased
158 muscle force (Fig. 2). Second, for a given Δt, greater values of Δx_m resulted in greater contraction
159 velocities. This reduced muscle force via $F_{velocity}$ (Eq. *3*). Given that contractions that caused larger
160 muscle excursions Δx_m increased force production by the spring and reduced force production by the
161 muscle (due to both F_{length} and $F_{velocity}$), the challenge was to determine, at every time step of the
162 simulation, which value of Δx satisfied Eq. *9*.

163 To satisfy all force, displacement, and velocity assumptions, we employed a numerical
164 technique that calculated F_{muscle} and F_{spring} for many values of Δx at each time step. Starting with the
165 first time step, we tested 5000 equally spaced Δx values corresponding to Δx_m (with units of fraction
166 of L_o) and plugged them into Eq. *9*, and thereby generated many hypothetical combinations of F_{muscle}
167 and F_{spring}. We then selected the value of Δx that resulted in the smallest difference between F_{muscle} and
168 F_{spring}. We repeated this numerical technique for all subsequent time steps until the muscle and spring
169 reached static equilibrium (i.e., when the change in muscle length between two time steps fell below an
170 arbitrary value of 0.0001 L_o).

171 ## *Inputs to the muscle-spring model*

172 ### *Muscle parameters*

173 Simulations of a bullfrog and grasshopper were conducted using parameter values for
174 components of the Hill-type model taken from previous studies (Table 1) (Bennet-Clark 1975; Azizi
175 and Roberts 2010; Sawicki, Sheppard, et al. 2015). In order to compare results from the bullfrog and
176 grasshopper, simulated contractions always started at the muscle resting length (bullfrog: L_o= 11.2 mm:
177 Sawicki et al. 2015; grasshopper: L_o= 4 mm: Bennet-Clark 1975), and all computed length changes

were converted to and reported as strain (i.e., $*L_o^{-1}$). The shape of $F_{activation}$, which was not reported in the literature, was approximated as a line with slope r_{act}. The slopes of r_{act} were chosen such that maximum activation occurred within biologically realistic muscle contraction times for both systems (within 100 to 300 ms). Based on published data, we estimated the duration of muscle contraction before the onset of jumping ($t_{contraction}$) as 50 ms in the bullfrog (Azizi and Roberts 2010) and 300 ms in the grasshopper (Bennet-Clark 1975).

Spring parameters

Two values of spring stiffness were defined: 1) the actual experimentally-measured spring stiffness of the tendon/apodeme-cuticular spring ($K_{bullfrog}$ or $K_{grasshopper}$ depending on the simulation) and 2) the values of spring stiffness used in the simulation to determine maximal energy storage ($k_{simulation}$). We estimated $K_{bullfrog}$ as 6.69 N/mm using published data from a fixed-end contraction (Sawicki, Robertson, et al. 2015). The spring system in grasshoppers was comprised of two springs in series, the apodeme (arthropod tendon) and the cuticular semilunar process. We calculated $K_{grasshopper}$ as the effective spring stiffness of these two springs (15.37 N/mm) using the following equation:

$$\mathrm{K_{grasshopper}} = \frac{K_{apodeme} \cdot K_{SLP}}{K_{apodeme} + K_{SLP}} \quad (10)$$

where $K_{apodeme}$ and K_{SLP} are the stiffness values of the apodeme (31.4 N/mm) and semilunar process (30 N/mm), respectively (Bennet-Clark 1975). The values of $k_{simulation}$ were uniformly generated from 5 to 350 $N*L_0^{-1}$ increments of 0.1 $N*L_0^{-1}$.

Simulation parameters

We simulated all muscle contractions with time steps of 0.001 s. The total number of steps was not determined before simulation. Instead, simulations terminated when change in muscle length reduced to less than 0.001 L_0^{-1} between time steps.

Identification of k_{maxE}

The determination of the spring stiffness that permitted maximal energy storage in the static

simulations was straightforward. The value of Δx in Eq. *8* was solved for many values of $k_{simulation}$. The stored energy for each simulation was calculated using Eq. *1*. The value of $k_{simulation}$ that resulted in the greatest stored energy was recorded as k_{maxE}.

Obtaining k_{maxE} from the dynamic muscle-spring model followed a similar process; however, the data required an additional pre-processing step. For each time step, Δx was calculated for various values of $k_{simulation}$ via Eq. 9.

To test the effect of muscle contraction duration ($t_{contraction}$), we ran simulations with truncated duration to exclude time steps that were greater than $t_{contraction}$. From the truncated dataset, k_{maxE} was determined using the methods above for the static and dynamic muscle-spring models.

Results

Static simulation

For both the bullfrog and the grasshopper, the amount of stored elastic energy was maximized for an intermediate spring stiffness (Fig. 4). As $k_{simulation}$ increased, stored energy rose, leveled off, and declined. In the bullfrog, the spring stiffness that permitted maximal energy storage (k_{maxE}; dotted lines in Fig. 4) equaled 21.10 N/mm, more than double the measured value of bullfrog tendon. The amount of energy stored with k_{maxE} and $K_{bullfrog}$ were 10.30 and 8.68 mJ, respectively (Table 2). In the grasshopper, k_{maxE} equaled 18.0 N/mm and the amount of energy stored with k_{maxE} and $K_{grasshopper}$ were 2.23 and 2.21 mJ, respectively (Table 2).

Dynamic simulations

As $t_{contraction}$ increased, more elastic energy was able to be stored. For example, maximal elastic energy stored at 50, 100, and 300 ms was 3.15, 8.16, and 8.68 mJ, respectively for the bullfrog and 0.03, 0.13, and 1.07 mJ for the grasshopper (Table 2). Also, all values resulting from the 5000 ms dynamic simulation matched those of the static simulation; therefore, because we reached the static steady-state solution by 5000 ms, we did not simulate muscle contraction past this time step.

Similar to the static simulation, dynamic simulations also revealed that an intermediate spring stiffness resulted in maximal stored energy; however, the value of k_{maxE} was dependent on $t_{contraction}$ (Figs. 3 & 4). Our simulation of the bullfrog muscle-spring system also showed that k_{maxE} was higher for faster rates of contraction (Fig. 3); therefore, as a point of comparison between the bullfrog and the grasshopper, unless otherwise stated, all reported results were taken from simulations at the highest r_{act} tested, resulting in tetanic contractions occurring in 100 ms.

In the bullfrog, k_{maxE} for a realistically time-limited contraction (50 ms) was 7.23 N/mm, less than half that predicted by the static solution (21.10 N/mm). This difference was a direct consequence of the force-velocity property of the frog muscle. Additionally, $K_{bullfrog}$ (7.93 N/mm) was much closer to k_{maxE} at 50 ms (7.23 N/mm) than to the k_{maxE} of the static simulation (21.10 N/mm). Alternatively, k_{maxE} in the grasshopper for a biologically relevant contraction duration (300 ms) was 18.0 N/mm, which matched the result predicted by the static solution (Table 2). Regardless of simulation, as $t_{duration}$ increased, so did k_{maxE} until the solution generated by the static solution was reached. This was shown by the rightward shift of the dotted line in Fig. 4 as time increased. When considering the highest value of r_{act} used in the simulations, k_{maxE} did not level out until 150 ms (Fig. 3). Additionally, the peak values of energy storage all occurred at the highest rates of activation (see Supplementary Material).

Discussion

By simulating the dynamic interaction between muscle and spring during a fixed-end contraction, we asked two questions: 1) Does reducing the time available for spring-loading affect which springs stored the most energy? 2) Do the values of spring stiffness in bullfrogs and grasshoppers permit maximum energy storage based on their contrasting loading regimes? For both the bullfrog and the grasshopper, the time available for muscle contraction determined which spring stiffness permitted maximal energy storage. As time restriction increased (i.e., as less time was available for muscle contraction), the values of spring stiffness that permitted maximal stored energy decreased (Fig. 4).

Although the greatest amounts of elastic energy were predicted using the static solution, this solution was not reached until 5000 ms in the grasshopper, a duration of muscle contraction that is much greater than what occurred in other experiments (Table 2). Consequently, static simulations may be insufficient to model muscle-spring systems in some cases. The static solution, however, offered an upper-bound of k_{maxE} and maximum stored energy in biological systems.

In both the bullfrog and the grasshopper, empirically-measured values of spring stiffness matched k_{maxE} when taking time-limited loading into account. In the bullfrog, dynamic simulation revealed that when the duration of muscle contraction was restricted to biologically-relevant contraction durations (50 ms), k_{maxE} and $K_{bullfrog}$ were similar (7.23 and 7.93 N/mm, respectively). Therefore, the incorporation of muscle dynamics into the simulation not only allowed the muscle-spring model to behave in a more realistic way, it countered the results of the static simulation and suggested that bullfrog tendons maximize energy storage at short timescales. Conversely, results from the dynamic simulation of the grasshopper muscle-spring system suggested that the grasshopper spring-system maximized energy at relatively long timescales. In the case of grasshoppers, which load their springs with longer durations than bullfrogs (300 ms and 50 ms, respectively), the static simulation provided reasonable estimates of k_{maxE} and maximal stored energy. These two cases demonstrated that biological springs can be loaded along a spectrum of durations and that muscle-spring system performance depended on the interaction between storage time available and muscle-spring properties.

The dynamic simulation of the bullfrog also demonstrated the importance of dynamics for all rates of muscle activation. At the fastest muscle activations, k_{maxE} did not level out until 150 ms (Fig. 3); therefore, bullfrog muscle-spring systems that complete energy storage within 150 ms are more sensitive to muscle dynamics than those that don't. Given that maximal *in vitro* activation of bullfrog muscle is reached in 100 ms (Sawicki, Sheppard, et al. 2015), this further demonstrated the importance

of muscle dynamics in bullfrog spring-systems.

The results of the dynamic simulations hinted at the importance of spring stiffness to fast muscle contractions. As muscle contraction duration decreases, the total amount of elastic energy that can be stored decreased (Fig. 4). Additionally, the sensitivity of k_{maxE} to muscle dynamics increased as the duration of muscle contraction decreased (Fig. 3). Therefore, in muscle-spring systems that are time-limited, properly tuning spring stiffness could help maximize energy in situations in which stored energy is decreased due to short contraction durations. In short, as muscle dynamics became more important, the optimal spring stiffness decreased.

Given that the results from the simulation were generated by connecting a Hill-type muscle model to a Hookean spring model, it is important to note the limitations of these constituent models in the context of this study. The Hill muscle model has been shown to accurately represent general trends in the relationship between the dynamics of muscle activation and force production (Cofer et al. 2010; Winters et al. 2011; Richards and Sawicki 2012). This relationship, however, was highly dependent on activation dynamics (Josephson 1985; Stevens 1996) and may not have been accurately represented in this study. Instead of focusing on the intricacies of neuronal firing, we simplified muscle activation as a linear ramp to test, in general, whether muscle activation rate affected time-limited energy storage. To that effect, the model demonstrated that muscle dynamics played a part in determining which spring stiffness permited maximal energy storage.

The results assumed that muscle contracts at rates such that maximal activation occurs within 100 ms. In reality, different jumps from the same animal could vary in muscle activation rate, thereby affecting the amount of spring stretch. The simulations show that bullfrog muscles that took longer than 100 ms to reach maximal activation stored less elastic energy for k_{maxE} (Fig. 3). Because the simulations were sensitive to variation in muscle activation rate, reported values of E_{max} and k_{maxE} should not be interpreted as exact predictions of optimal bullfrog performance. Nonetheless, these

297 values do provide a qualitative view of how muscle and spring parameters interact during time-limited
298 energy storage.

299 Another simplification of the model involved the use of a linear spring. Most biological
300 structures, including bullfrog tendons, exhibit a toe-region of low spring stiffness early in the force-
301 displacement curve followed by a linear region of higher spring stiffness. Many studies remedy this by
302 measuring spring stiffness in the linear region of the force-displacement curve. Also, it is important to
303 note that the simulation only predicted the amount of energy stored, but other factors such as mass,
304 material properties, and morphological lever systems directly impact the unloading of energy
305 (McHenry et al. 2012; Anderson et al. 2014).

306 Our dynamic simulations revealed a phenomenon that potentially affects all spring systems that
307 are transiently loaded by muscle. That is, muscles that can't develop isometric force because of time
308 restriction can achieve significant amounts of elastic energy storage when coupled with springs of
309 lower stiffness than would be predicted in the static case. For example, because bullfrogs lack
310 morphological latches, they are not able to load their springs with peak isometric force. Instead, the
311 bullfrog uses a dynamic catch mechanism, which temporarily resists force via inertial loads and
312 mechanical advantage about moving joints (Astley and Roberts 2014). The dynamic catch is able to
313 resist some muscle contraction to permit spring loading, but not long enough for isometric contractions
314 to develop. With the exception of salamanders, which contain anatomical latches (Deban et al. 2007), it
315 is likely that vertebrates are inherently subject to time-limited energy storage and potentially benefit
316 from springs less stiff than expected.

317 Conversely, we predict that some invertebrate systems with anatomical latches may operate
318 with relatively higher spring stiffness that can permit maximal energy storage over long storage times.
319 Systems that have anatomical latches, and those that use rigid connections of body parts to resist
320 muscle contraction, can develop isometric contractions during spring loading. For example, both the

snapping shrimp (*Alpheus californiensis*) and froghopper (*Philaenus spumarius*) contain body parts that lock together to form a latch and have springs that are connected to slow, forceful muscles that contract isometrically for several seconds (Ritzmann 1973; Ritzmann 1974; Burrows 2007). Given the amount of power-amplification observed in these systems, it is likely that these muscle-spring systems are operating with values of spring stiffness that permit maximal energy storage.

In some invertebrate systems, the determination of an optimal spring stiffness can be complicated by an active latch, in which an antagonist muscle contracts to keep a system latched. Active latches may permit variation in the amount of stored energy prior to movement(Burrows and Morris 2001; Burrows 2003; Kagaya and Patek 2016). For example, the bush cricket can use changes in both joint angle and activation of the latching muscle to determine how much force holds the latch in place (Burrows 2003). Meanwhile, a larger muscle can load the spring until it exceeds the force of the latch, thereby initiating movement. Given that the bush cricket can control the amount of energy stored, it is possible that it operates with a spring stiffness that results in the most stored energy for a wide range of situations. Although this idea is speculative, this study provides the tools necessary to test this hypothesis in other active latch systems in future work.

Conclusion

When testing for maximal energy storage, it is important to consider the dynamic interaction of muscle and spring. Our simulations revealed that within the realm of biologically relevant timescales, the more time available for loading by muscle, the stiffer the series spring required for maximum elastic energy storage. Muscles that load in-series springs over shorter timescales benefit from less stiff springs. At short timescales, muscle force is small due to low activation and high velocity, and less stiff springs allow the spring to stretch more for a given amount of force. Thus, it is necessary to determine the effect, if any, of muscle dynamics on energy storage before concluding whether or not muscle-spring systems maximize energy storage.

345

Ethics

346 All animal information was based on previously published datasets.
347
348

Data accessibility

349 All R code used for simulations can be found at https://github.com/mrosario/muscle-springSimulation.
350 Data generated from the simulation have been uploaded to Dryad
351 (http://dx.doi.org/10.5061/dryad.j4k89).
352
353

Competing interests

354 We have no competing interests.
355
356

Authors' contributions

357 MVR implemented the mathematical model, ran all dynamic simulations, analyzed the data, and
358 prepared the manuscript, GPS conceived the original idea of the static model and guided the study to
359 include grasshoppers, SNP helped prepare the manuscript and identified key points/questions of the
360 study, GSS helped develop the dynamic model and simulations, provided data from bullfrogs, offered
361 insight on data analysis/interpretation and helped edit the manuscript.
362
363

Acknowledgments

364 The authors would like to thank E. Azizi for providing feedback on the manuscript. We also appreciate
365 comments and contributions from P. Green, P.S.L. Anderson, K. Kagaya, R. Crane. We thank the DOE
366 CSGF for training provided for high speed computing.
367
368
369

Funding

370 This research was funded by grants awarded to M.V. Rosario (DOE FG02-97ER25308) and S.N. Patek
371 (NSF IOS-1439850).

References

Anderson PSL, Claverie T, Patek SN. 2014. Levers and linkages: Mechanical trade-offs in a power-amplified system. Evolution (N. Y). 68:1919–1933.

Astley HC, Roberts TJ. 2014. The mechanics of elastic loading and recoil in anuran jumping. J. Exp. Biol. 217:4372–4378.

Azizi E, Roberts TJ. 2010. Muscle performance during frog jumping: influence of elasticity on muscle operating lengths. Proc. Biol. Sci. 277:1523–1530.

Bennet-Clark HC. 1975. The energetics of the jump of the locust *Schistocerca gregaria*. J. Exp. Biol. 63:53–83.

Burrows M. 2003. Jumping and kicking in bush crickets. J. Exp. Biol. 206:1035–1049.

Burrows M. 2007. Neural control and coordination of jumping in froghopper insects. J. Neurophysiol. 97:320–330.

Burrows M, Morris G. 2001. The kinematics and neural control of high-speed kicking movements in the locust. J. Exp. Biol. 204:3471–81.

Cofer D, Cymbalyuk G, Reid J, Zhu Y, Heitler WJ, Edwards DH. 2010. AnimatLab: a 3D graphics environment for neuromechanical simulations. J. Neurosci. Methods 187:280–8.

Deban SM, O'Reilly JC, Dicke U, van Leeuwen JL. 2007. Extremely high-power tongue projection in plethodontid salamanders. J. Exp. Biol. 210:655–667.

Hill AV. 1938. The heat of shortening and the dynamic constants of muscle. Proc. R. Soc. B Biol. Sci. 126:136–195.

Hollinger JO. 2011. An Introduction to Biomaterials. Second edition. CRC Press.

Josephson RK. 1985. Mechanical power output from striated muscle during cyclic contraction. J. Exp. Biol. 114:493–512.

Kagaya K, Patek SN. 2016. Motor control of ultrafast, ballistic movements. J. Exp. Biol.:319–333.

Marsh RL, John-Alder HB. 1994. Jumping performance of hylid frogs measured with high-speed cine film. J. Exp. Biol. 188:131–141.

McHenry MJ, Claverie T, Rosario M V, Patek SN. 2012. Gearing for speed slows the predatory strike of a mantis shrimp. J. Exp. Biol. 215:1231–45.

Patek S, Rosario M V, Taylor J. 2013. Comparative spring mechanics in mantis shrimp. J. Exp. Biol. 216:1317–29.

Peplowski MM, Marsh RL. 1997. Work and power output in the hindlimb muscles of Cuban tree frogs *Osteopilus septentrionalis* during jumping. J. Exp. Biol. 200:2861–2870.

Richards CT, Sawicki GS. 2012. Elastic recoil can either amplify or attenuate muscle-tendon power, depending on inertial vs. fluid dynamic loading. J. Theor. Biol. 313:68–78.

Ritzmann R. 1973. Snapping behavior of the shrimp *Alpheus californiensis*. Science 181:459–460.

Ritzmann R. 1974. Mechanisms for the snapping behavior of two alpheid shrimp, *Alpheus californiensis* and *Alpheus heterochelis*. J. Comp. Physiol. 95:217–236.

Roberts TJ, Marsh RL. 2003. Probing the limits to muscle-powered accelerations: lessons from

411 jumping bullfrogs. J. Exp. Biol. 206:2567–2580.

412 Rosario M V, Patek SN. 2015. Multilevel analysis of elastic morphology: The mantis shrimp's spring.
413 J. Morphol. 276:1123 – 1135.

414 Sawicki GS, Robertson BD, Azizi E, Roberts TJ. 2015. Timing matters: tuning the mechanics of a
415 muscle–tendon unit by adjusting stimulation phase during cyclic contractions. J. Exp. Biol. 218:3150–
416 3159.

417 Sawicki GS, Sheppard P, Roberts TJ. 2015. Power amplification in an isolated muscle-tendon is load
418 dependent. J. Exp. Biol.:3700–3709.

419 Stevens ED. 1996. The pattern of stimulation influences the amount of oscillatory work done by frog
420 muscle. J. Physiol. 494:279–285.

421 Wilson AM, Watson JC, Lichtwark G a. 2003. Biomechanics: A catapult action for rapid limb
422 protraction. Nature 421:35–36.

423 Winters J. 1990. Hill-based muscle models: a systems engineering perspective. In: Multiple Muscle
424 Systems: Biomechanics and Movement Organization. p. 69–93.

425 Winters TM, Takahashi M, Lieber RL, Ward SR. 2011. Whole muscle length-tension relationships are
426 accurately modeled as scaled sarcomeres in rabbit hindlimb muscles. J. Biomech. 44:109–15.

427 Zajac FE. 1989. Muscle and tendon: properties, models, scaling, and application to biomechanics and
428 motor control. Crit. Rev. Biomed. Eng. 17:359–411.

429 Zajac FE, Gordon ME. 1989. Determining muscle's force and action in multi-articular movement.
430 Exerc. Sport Sci. Rev. 17:187–230.

431

432

Figure and Table Captions

Table 1. Muscle parameters that were used to create the muscle-spring system were from previously published data. Together, these parameters define the length-tension and force-velocity relationships of contracting muscle of bullfrogs and grasshoppers. Bennet-Clark 1975 [(a)]; Azizi and Roberts 2010 [(b)]; Sawicki, Sheppard, et al. 2015 [(c)].

Table 2. As the duration of muscle contraction approaches biologically-relevant durations (bold), k_{maxE} becomes closer to the measured spring stiffness ($K_{bullfrog}$ and $K_{grasshopper}$). Static simulations accurately model systems that exhibit relatively long loading times such as the grasshopper (grey background). Dynamic simulations are necessary for systems that exhibit time-limited contraction such as the bullfrog (white background).

Figure 1. During a fixed-end contraction of a muscle-spring system, the stored elastic energy depends on spring stiffness and the force the muscle generates. **A)** At rest, the maximum force the muscle can generate (red circle) is much higher than the force of the spring (blue circle). While the muscle contracts, maximum muscle force (red line) decreases due to the muscle's length-tension properties, and the spring is stretched, thereby increasing spring force. Maximum contraction is reached when maximum muscle force and spring force coincide. **B)** When given infinite time for contraction, all spring systems reach maximum contraction and intersect with the muscle's length-tension curve (red line). In this example, the stored energy (area of the triangle formed) is higher in the stiffer spring system (light blue) than the more compliant system (dark blue). **C)** This relationship changes, however, when contraction duration is reduced to 75 ms because the muscle doesn't reach maximum contraction in this duration. At this shortened duration, the less stiff spring system (dark blue) stores more energy. Although this demonstration provides proof-of-concept, this relationship remains to be found in biological systems prior to the present study.

458 Figure 2. In the Hill-type muscle model, force depends on three components: length, velocity, and
459 activation. The contributions of each component are mathematically defined in Eq. 2 - 4. Each plot was
460 generated using properties of bullfrog plantaris longus muscle.
461
462 Figure 3. Regardless of activation rate, the spring stiffness that permits maximal energy storage (k_{maxE})
463 is dependent on the duration of muscle contraction ($t_{contraction}$). For example, k_{maxE} at 300 ms
464 (approximating the static, steady state) is higher than k_{maxE} measured at 50 and 100 ms. For fast
465 activations, k_{maxE} is more sensitive at smaller durations of muscle contraction, demonstrated by the
466 large slope. The fast, intermediate, and slow activations reach maximum activation within 100, 200,
467 and 300 ms, respectively. Data shown are from the bullfrog model.

468 Figure 4. The duration of muscle contraction ($t_{contraction}$) determines whether the spring stiffness of
469 bullfrog tendon ($K_{bullfrog}$, indicated by arrow) permits maximal energy storage. For example, in the
470 static simulation, $K_{bullfrog}$ does not coincide with the peak of the curve (indicated by dotted line).
471 Results from the static simulation suggest that $K_{bullfrog}$ does not permit maximal energy storage.
472 Conversely, during time-limited muscle contractions (50 ms), $K_{bullfrog}$ is closer to the peak of the curve.
473 The leftward shift of the peak as $t_{contraction}$ is reduced suggests that muscle-spring dynamics become
474 increasingly important with shorter durations of muscle contraction. Conversely, in grasshoppers, the
475 static solution is a close approximation of the results from the biologically-relevant loading time (300
476 ms). Results from simulations that occur at biologically-relevant loading times are boxed. Note that the
477 scale of y axes is different in each panel.
478

Tables

Table 1. Muscle parameters that were used to create the muscle-spring system were from previously published data. Together, these parameters define the length-tension and force-velocity relationships of contracting muscle of bullfrogs and grasshoppers. Bennet-Clark 1975 [(a)]; Azizi and Roberts 2010 [(b)]; Sawicki, Sheppard, et al. 2015 [(c)].

Parameter	Value for bullfrog	Value for grasshopper	Definition
F_{max}	42.7 N [(c)]	13.1 N [(a)]	Maximum tetanic force
v_{max}	124.1 mm/s [(c)]	7.0 mm/s [(a)]	Maximum contraction velocity
L_0	11.2 mm [(c)]	4.0 mm [(a)]	Resting length of muscle
$t_{contraction}$	100 ms [(c)]	300 ms [(a)]	Time until maximum *in vitro* muscle activation
a_L	2.08 [(b)]	2.08 [(b)]	Determines shape of length-tension relationship
b_L	-2.89 [(b)]	-2.89 [(b)]	Determines shape of length-tension relationship
s	-.75 [(b)]	-.75 [(b)]	Determines shape of length-tension relationship
mass	213.9 – 373.0 g [(c)]	1.5 – 2.0 g [(a)]	Range of body mass

Table 2. As the duration of muscle contraction approaches biologically-relevant durations (bold), k_{maxE} becomes closer to the measured spring stiffness ($K_{bullfrog}$ and $K_{grasshopper}$). Static simulations accurately model systems that exhibit relatively long loading times such as the grasshopper (grey background). Dynamic simulations are necessary for systems that exhibit time-limited contraction such as the bullfrog (white background).

	Bullfrog				Grasshopper			
$t_{contraction}$ (ms)	k_{maxE} (N/mm)	$K_{bullfrog}$ (N/mm)	E_{max} (mJ)	$E_{bullfrog}$ (mJ)	k_{maxE} (N/mm)	$K_{grasshopper}$ (N/mm)	E_{max} (mJ)	$E_{grasshopper}$ (mJ)
50	**7.23**	**7.93**	**3.15**	**3.09**	6.5	15.37	0.36	0.33
100	16.43	7.93	8.16	7.60	6.75	15.37	0.14	0.13
200	21.06	7.93	10.29	8.68	8.75	15.37	0.53	0.51
300	21.11	7.93	10.30	8.68	**12.0**	**15.37**	**1.08**	**1.07**
5000	21.11	7.93	10.30	8.68	18.0	15.37	2.24	2.21
static	21.11	7.93	10.30	8.68	18.0	15.37	2.24	2.21

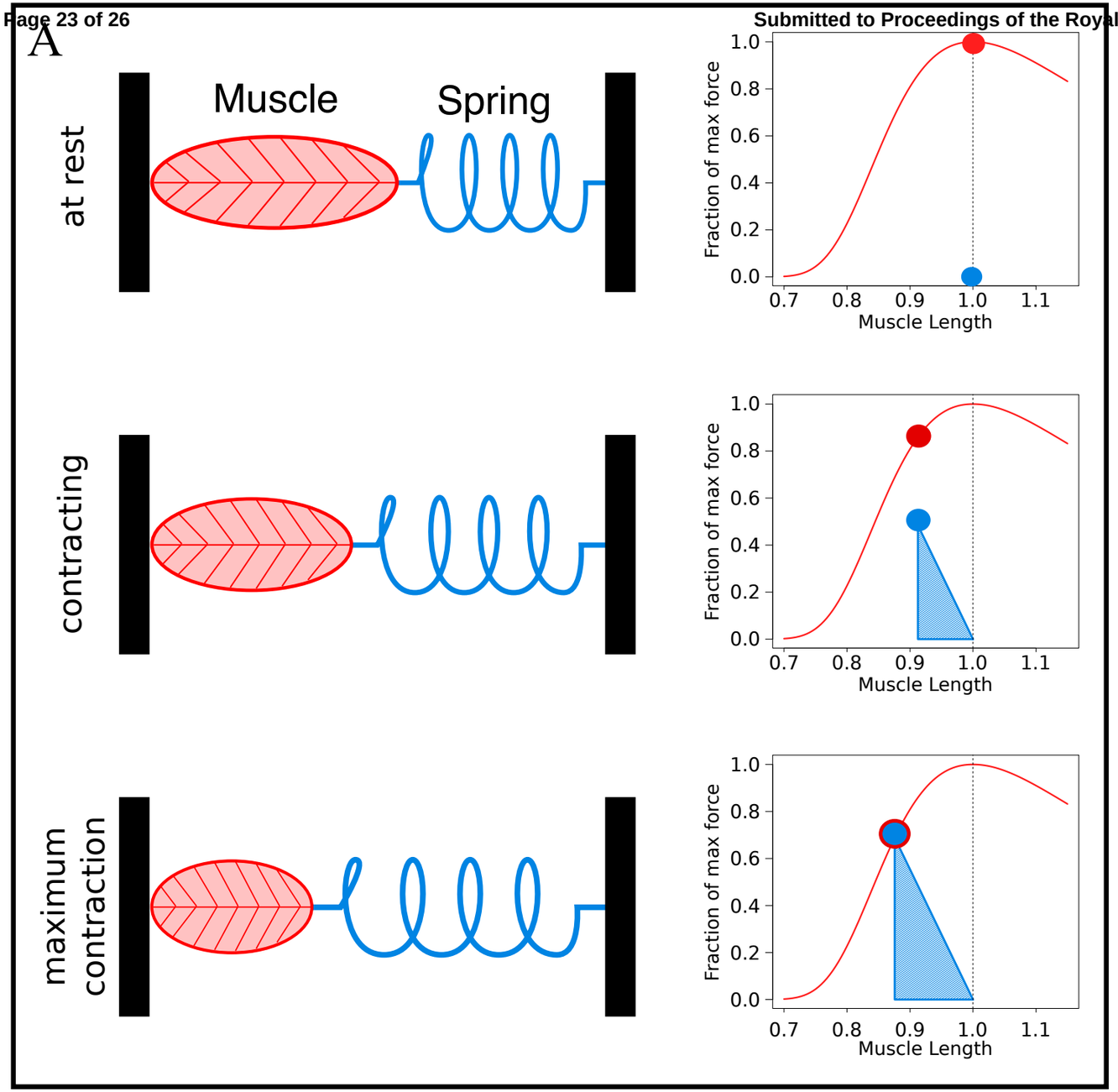

Figure 1. During a fixed-end contraction of a muscle-spring system, the stored elastic energy depends on spring stiffness and the force the muscle generates. **A)** At rest, the maximum force the muscle can generate (red circle) is much higher than the force of the spring (blue circle). While the muscle contracts, maximum muscle force (red line) decreases due to the muscle's length-tension properties, and the spring is stretched, thereby increasing spring force. Maximum contraction is reached when maximum muscle force and spring force coincide. **B)** When given infinite time for contraction, all spring systems reach maximum contraction and intersect with the muscle's length-tension curve (red line). In this example, the stored energy (area of the triangle formed) is higher in the stiffer spring system (light blue) than the more compliant system (dark blue). **C)** This relationship changes, however, when contraction duration is reduced to 75 ms because the muscle doesn't reach maximum contraction in this duration. At this shortened duration, the less stiff spring system (dark blue) stores more energy. Although this demonstration provides proof-of-concept, this relationship remains to be found in biological systems.

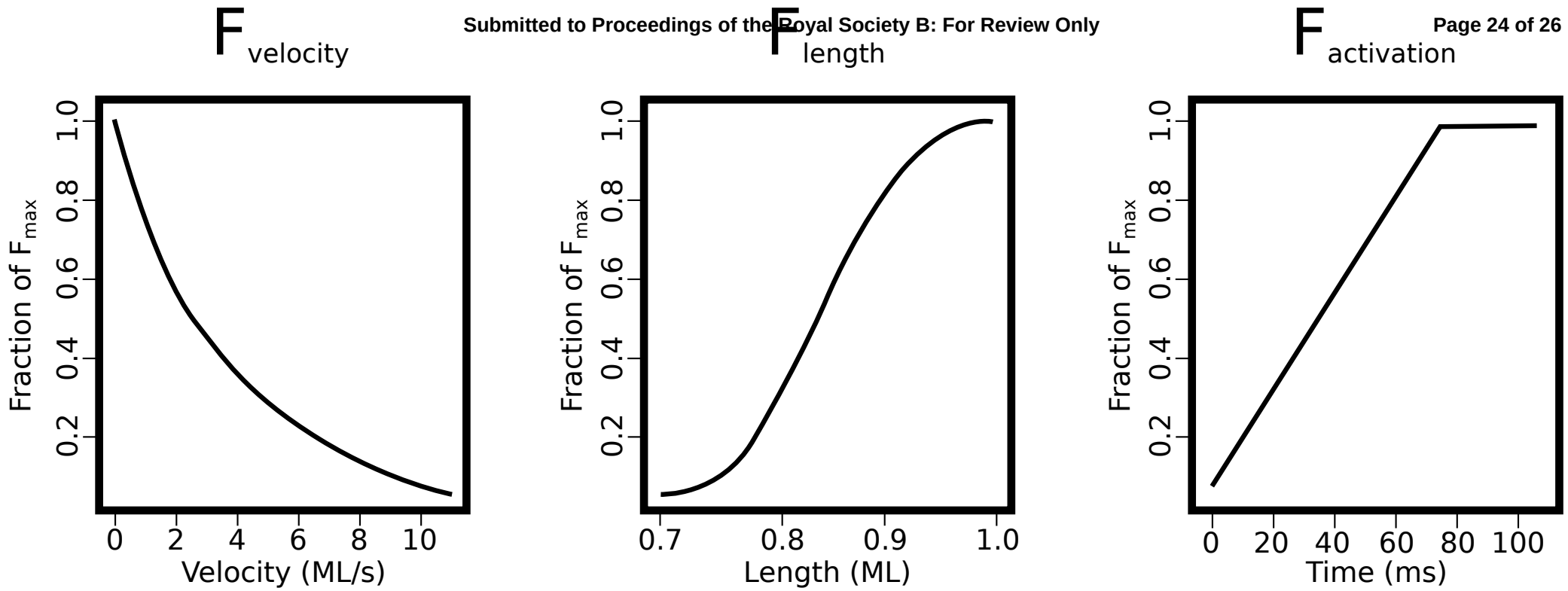

Figure 2. In the Hill-type muscle model, force depends on three components: length, velocity, and activation. The contributions of each component are mathematically defined in Eqs 2–4. Each plot was generated using properties of bullfrog plantaris longus muscle.

Submitted to Proceedings of the Royal Society B: For Review Only

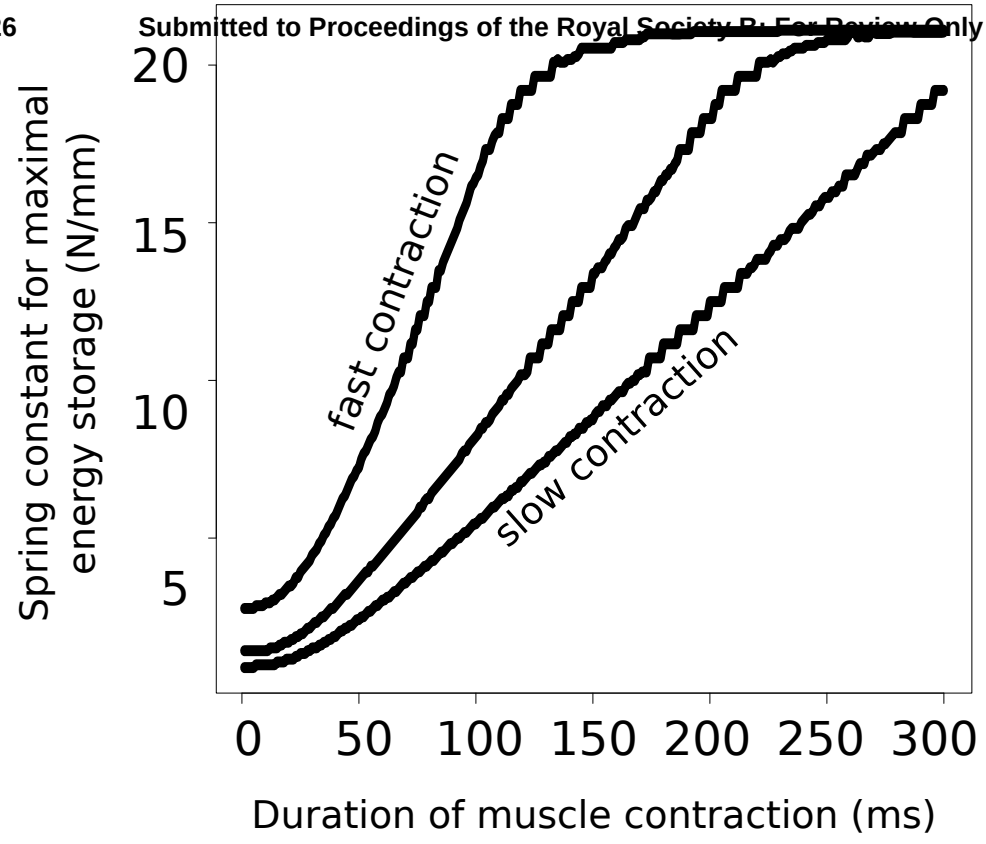

Figure 3. Regardless of activation rate, the spring stiffness that permits maximal energy storage (kmaxE) is dependent on the duration of muscle contraction (tcontraction). For example, kmaxE at 300 ms (approximating the static, steady state) is higher than kmaxE measured at 50 and 100 ms. For fast activations, kmaxE is more sensitive at smaller durations of muscle contraction, demonstrated by the large slope. The fast, intermediate, and slow activations reach maximum activation within 100, 200, and 300 ms, respectively. Data shown are from the bullfrog model.

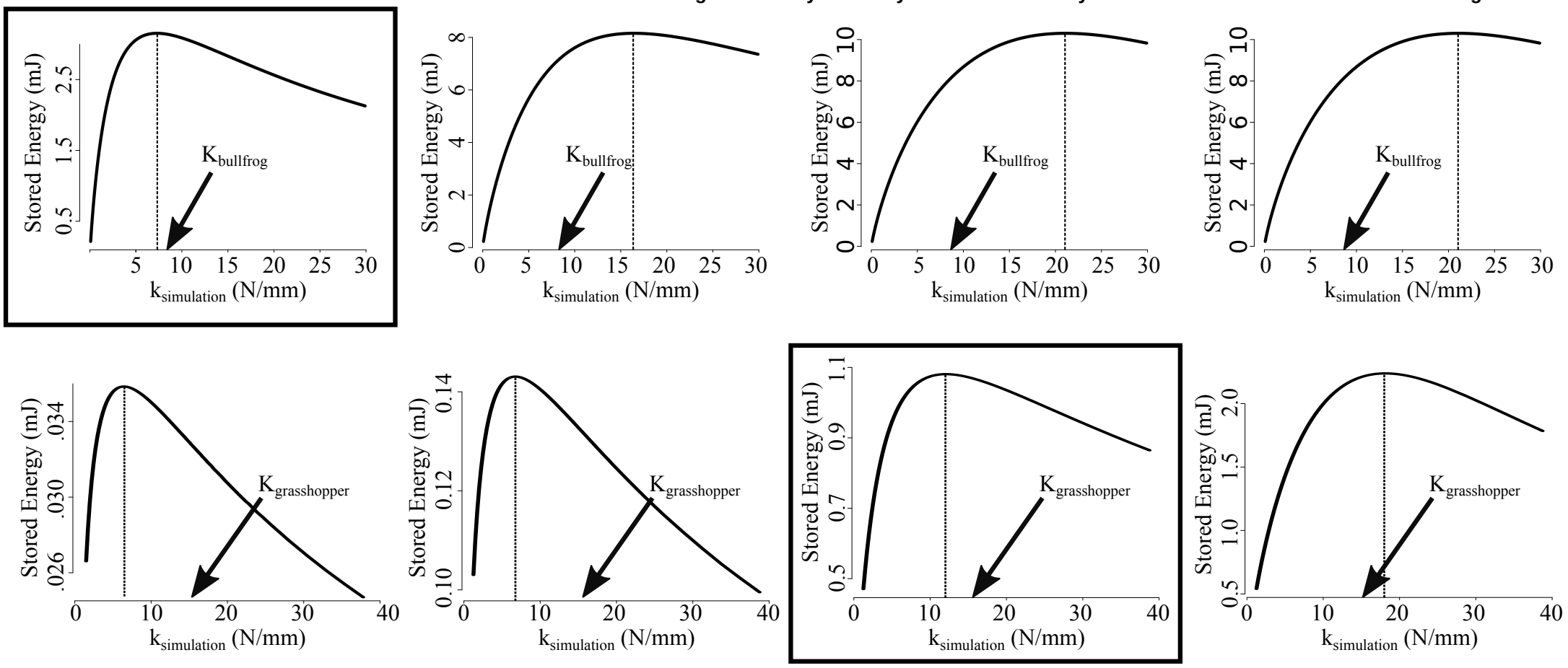

Figure 4. The duration of muscle contraction (tcontraction) determines whether the spring stiffness of bullfrog tendon (Kbullfrog, indicated by arrow) permits maximal energy storage. For example, in the static simulation, Kbullfrog does not coincide with the peak of the curve (indicated by dotted line). Results from the static simulation suggest that Kbullfrog does not permit maximal energy storage. Conversely, during time-limited muscle contractions (50 ms), Kbullfrog is closer to the peak of the curve. The leftward shift of the peak as tcontraction is reduced suggests that muscle-spring dynamics become increasingly important with shorter durations of muscle contraction. Conversely, in grasshoppers, the static solution is a close approximation of the results from the biologically-relevant loading time (300 ms). Results from simulations that occur at biologically-relevant loading times are boxed. Note that the scale of y axes is different in each panel.